Current instability, limit cycles, and entropy production surface

Jaleel Ali and Byung Chan Eu

Citation: The Journal of Chemical Physics **81**, 4401 (1984); doi: 10.1063/1.447407
View online: http://dx.doi.org/10.1063/1.447407
View Table of Contents: http://scitation.aip.org/content/aip/journal/jcp/81/10?ver=pdfcov
Published by the AIP Publishing

Current instability, limit cycles, and entropy production surface[a)]

Jaleel Ali and Byung Chan Eu
Department of Chemistry, McGill University, 801 Sherbrooke St. W., Montreal, P.Q., Canada H3A 2K6

(Received 1 February 1984; accepted 11 June 1984)

A phenomenological model for the evolution equations for charged carriers in semiconductors is proposed which can give rise to a limit cycle of current as the field strength passes through a critical point. The model is a modification of the previously reported model for carrier mobility. We have studied the macroscopic dynamics of the model and its relation to the structure of the entropy production surface corresponding to the model, by solving the evolution equations by a numerical method. It is found that when a limit cycle appears as a solution the average entropy production over a cycle tends to decrease, compared with that of the unstable steady state from which the limit cycle has bifurcated. Based on the study made, we propose a conjecture on a relationship between the trajectories of a macroscopic evolution and the structure of the entropy production surface.

I. INTRODUCTION

Temporal and spatial evolutions of macroscopic processes in nature are described generally by a set of nonlinear (partial or ordinary) differential equations[1] for macroscopic variables such as the density, internal energy, momentum, stress tensors, heat fluxes, etc. Steady states of such a system of differential equations and their stability are often important for understanding the dynamics of the system under study. Stability of nonlinear dynamical systems may be studied by means of the Lyapounov function,[2] but the problem with the Lyapounov second method is in the difficulty of constructing the Lyapounov function for the system of interest. Therefore, although the method is attractive in principle, it has not proven practical for irreversible thermodynamics for systems removed far from equilibrium.

Chemists are accustomed to think of a chemical reaction as a dynamical event occurring on a potential energy surface[3] provided by the electrons in the atoms comprising the reacting system, the potential energy surface in turn supplying the force field for the event, and in the case of such a force field the classical dynamical equations of motion are generally nonlinear. The geometrical structure of a potential energy surface aids the chemist to guess, at least, qualitatively and roughly the outcome of the chemical reaction and the classical trajectories. It is fair to say that the idea of potential energy surface has been a very useful one in chemistry, helping the chemist sort out and see through a maze of complicated chemical phenomena. The potential energy surface has some aspects in it that are reminiscent of the Lyapounov functions in nonlinear mathematics, although the analogy is not perfect and one should not be confused by a similarity.

Unlike a microscopic chemical reaction occurring on a potential energy surface, the evolution of a macroscopic variable is subject to constraints[1] of thermodynamic laws. Especially, the second law of thermodynamics plays an essential role by restricting the acceptable forms for the evolution equations for nonconserved variables such as heat fluxes $\mathbf{Q}_i'$, diffusion fluxes $\mathbf{J}_i$, and stress tensors $\overleftrightarrow{P}_i$, etc. If such evolution equations are collectively denoted by the equation[1]

$$\rho \frac{d}{dt} \hat{\Phi}_i^{(\alpha)} = \hat{Z}_i^{(\alpha)} + \Lambda_i^{(\alpha)}, \quad i,\alpha = 1,2,3,..., \tag{1.1a}$$

where ρ is the mass density, $\hat{\Phi}_i^{(\alpha)}$ the flux density of the αth flux for species i: $(\Phi_i^{(\alpha)} = \rho\hat{\Phi}_i^{(\alpha)}$; $\Phi_i^{(1)} = \frac{1}{2}(\overleftrightarrow{P}_i + \overleftrightarrow{P}_i^t) - \frac{1}{3}\overleftrightarrow{U}\,\mathrm{tr}\,\overleftrightarrow{P}_i$, $\Phi_i^{(2)} = \frac{1}{3}\,\mathrm{tr}\,\overleftrightarrow{P}_i - p_i$, $\Phi_i^{(3)} = \mathbf{Q}_i'$, $\Phi_i^{(4)} = \mathbf{J}_i$,...; p_i = hydrostatic pressure), $Z_i^{(\alpha)}$ the convective term containing the thermodynamic driving force responsible for the flux (see Table I for various forms for them), and $\Lambda_i^{(\alpha)}$ the so-called dissipative term which may be a nonlinear function of the fluxes. The flux evolution equations (1.1a) are coupled to the conservation laws (balance equations) of mass, momentum, and internal energy:

$$\frac{\partial}{\partial t}\rho = -\,\mathrm{div}\,\rho\mathbf{u}, \tag{1.1b}$$

$$\rho \frac{d}{dt} c_i = -\,\mathrm{div}\,\mathbf{J}_i + \Lambda_i^{(0)}, \tag{1.1c}$$

$$\rho \frac{d}{dt}\mathbf{u} = -\,\mathrm{Div}\,\overleftrightarrow{P} + \rho_e\mathbf{E}, \tag{1.1d}$$

$$\rho \frac{d}{dt}\mathscr{E} = -\,\mathrm{div}\,\mathbf{Q} - \overleftrightarrow{P}{:}\mathrm{Grad}\,\mathbf{u} + \mathbf{J}_e\cdot\mathbf{E}, \tag{1.1e}$$

where

$\mathbf{E}$ = external electric field,

$\mathbf{u}$ = velocity of the fluid,

$\mathscr{E}$ = internal energy of the fluid,

ρ_i = mass density of species i,

$$\rho = \sum_i \rho_i,$$

$$\rho_e = \sum_i z_i \rho_i,$$

$$c_i = \rho_i/\rho,$$

$$\mathbf{J}_e = \sum_i z_i \mathbf{J}_i,$$

$$\overleftrightarrow{P} = \sum_i \overleftrightarrow{P}_i,$$

$$\mathbf{Q}_i' = \mathbf{Q}_i - \hat{h}_i \mathbf{J}_i,$$

$$\mathbf{Q} = \sum_i \mathbf{Q}_i,$$

[a)] Work supported by the grants from the Natural Sciences and Engineering Research Council of Canada.

TABLE I. Formulas for $Z_i^{(\alpha)}$.

α	$Z_i^{(\alpha)}$
(1)	$-\nabla\cdot\psi_i^{(1)} + 2[\overleftrightarrow{P}_i \cdot \text{Grad}\,\mathbf{u}]^{(2)} - 2[\mathbf{J}_i(d\mathbf{u}/dt)]^{(2)} + 2[\mathbf{J}_i\mathbf{F}_i]^{(2)}$
(2)	$-\nabla\cdot\psi_i^{(2)} - \frac{2}{3}(\overleftrightarrow{P}_i - p_i\overleftrightarrow{U})$:Grad $\mathbf{u} - \frac{2}{3}\mathbf{J}_i\cdot(d\mathbf{u}/dt) - p_i[d\ln(p_i v^{5/3})/dt] + \frac{2}{3}\mathbf{J}_i\cdot\mathbf{F}_i$
(3)	$-\nabla\cdot\psi_i^{(3)} - [(d\mathbf{u}/dt) - \mathbf{F}_i]\cdot(\overleftrightarrow{P}_i - p_i\overleftrightarrow{U}) - \mathbf{Q}_i'\cdot\text{grad}\,\mathbf{u} - \varphi_i^{(3)}\cdot\text{Grad}\,\mathbf{u}$ $- \mathbf{J}_i(d\hat{h}_i/dt) - \overleftrightarrow{P}_i\,\text{grad}\,\hat{h}_i$
(4)	$-\text{Div}\,\overleftrightarrow{P}_i + c_i\,\text{Div}\,\overleftrightarrow{P} - \mathbf{J}_i\cdot\text{Grad}\,\mathbf{u} + \rho_i(\mathbf{F}_i - \mathbf{F})$

$\mathbf{F}_i$ is the external force on uniy mass of i.

$\mathbf{F} = \sum_i c_i\mathbf{F}_i$.

$[\overleftrightarrow{A}]^{(2)}$ stands for the traceless symmetric part of the second rank tensor $\overleftrightarrow{A}$. For $\psi_i^{(\alpha)}$ and $\varphi_i^{(3)}$ see Ref. 1. They are moments of peculiar velocity and may be expressed in terms of conserved and nonconserved variables, i.e., mass density, momentum, concentrations, internal energy or temperature, mass fluxes, heat fluxes, and stress tensors.

$\hat{h}_i$ = enthalpy density per unit mass of i,

$\Lambda_i^{(0)}$ = reaction rate for species i (source terms).

We must append to the Eqs. (1.1a)–(1.1e) the entropy balance equation

$$\rho\frac{d}{dt}\mathscr{S} = -\text{div}\,\mathbf{J}_s + \sigma\,, \tag{1.1f}$$

where $\mathscr{S}$ is the entropy density, $\mathbf{J}_s$ the entropy flux, and σ the entropy production. It is necessary to add the entropy balance equation in order to make the macroscopic processes described by Eqs. (1.1a)–(1.1e) consistent with the thermodynamic laws as they should, since the entropy balance equation is a dynamic expression for the second law of thermodynamics to which all macroscopic processes must be rigorously subjected. This is a distinguishing feature of the theory of nonlinear irreversible processes developed in a series of papers by one of us, and the present paper is a part of the endeavor. However, in many practical cases including present problem the fluxes (nonconserved variables) evolve on a faster time scale than the conserved variables such as density or mass fractions, momentum, and internal energy. In such cases it is appropriate to solve the evolution equations (1.1a) adiabatically keeping the slowly varying conserved variables in them fixed as a function of time and position. In other words, the evolution equations (1.1a) are first solved separately from the balance equations (1.1b)–(1.1e). Then the solutions of the evolution equations are put into the balance equations to obtain generalized hydrodynamic equations which are solved subject to initial and boundary conditions appropriate for the problem in hand. This separation procedure will be called the adiabatic approximation and will be used in the present paper.

Since the second law of thermodynamics is represented by the positive entropy production, acceptable forms for the dissipative terms are restricted by the requirement by the second law in the following manner. Let $X_i^{(\alpha)}$ be functions of the fluxes as well as the conserved variables. Then, the dissipative terms $\Lambda_i^{(\alpha)}$ must be such that[1]

$$\sum_i X_i^{(\alpha)}\odot\Lambda_i^{(\alpha)} \geqslant 0\,. \tag{1.2}$$

In fact, it can be shown that if the entropy production is given by the form below [see Eq. (1.5) below] and if $X_i^{(\alpha)}$ obey a certain set of consistency conditions[1] there follows from Eqs. (1.1a)–(1.1e) a differential form for the entropy density

$$Td\mathscr{S} = d\hat{\mathscr{E}} + pdv - \sum_i c_i z_i d\phi - \sum_i \hat{\mu}_{ei}dc_i + \sum_{i\alpha} X_i^{(\alpha)}\odot d\hat{\Phi}_i^{(\alpha)}\,, \tag{1.3}$$

where v is the specific volume and ϕ is the potential of $\mathbf{E}$, and

$$\hat{\mathscr{E}} = \mathscr{E} + z\phi\,,$$

$$z = \sum_i c_i z_i\,,$$

$$\hat{\mu}_{ei} = \mu_{ei}/m_i = \mu_i/m_i + z_i\phi\,,$$

μ_i being the chemical potential of i. Therefore, $\hat{\mu}_{ei}$ is seen to be the electrochemical potential per unit mass of i. The differential form (1.3) also implies that $X_i^{(\alpha)}$ are the entropy derivatives with respect to the fluxes $\hat{\Phi}_i^{(\alpha)}$:

$$T^{-1}X_i^{(\alpha)} = (\partial\mathscr{S}/\partial\hat{\Phi}_i^{(\alpha)})\,, \tag{1.4}$$

where T is the temperature. The kinetic theory consideration based on the modified moment method suggests that the entropy production σ due to the irreversible processes corresponding to $\hat{\Phi}_i^{(\alpha)}$ is given by

$$\sigma = T^{-1}\sum_{i\alpha} X_i^{(\alpha)}\odot\Lambda_i^{(\alpha)} = \sum_{i\alpha}(\partial\mathscr{S}/\partial\hat{\Phi}_i^{(\alpha)})\odot\Lambda_i^{(\alpha)}\,. \tag{1.5}$$

The above set of equations forms the general framework of the theory of nonlinear irreversible processes developed previously, and as shown in other examples for its application to some practical problems,[4–7] the theory is an extension of linear irreversible thermodynamics and provides a fairly general means to handle diverse nonlinear macroscopic processes.

The entropy production is not only a positive quantity, but also a surface in the space defined by $\{\sigma, \hat{\Phi}_i^{(\alpha)}; i,\alpha = 1,2,3,\ldots\}$ on which the macroscopic processes evolve according to the dictate of the evolution equations subject to the initial conditions. We call the path of macroscopic processes in the space the trajectory, and this trajectory remains on the entropy production surface for processes consistent with the second law of thermodynam-

ics. In this sense the role of entropy production surface is quite akin to the potential energy surface in a chemical reaction. (There is one important distinction to be made between the potential energy surface and the entropy production surface, however. That is, while the force field is tangential to the potential energy surface in the case of chemical reactions, the dissipative terms $\Lambda_i^{(\alpha)}$ are generally not tangential to the entropy production surface except for the case of a linear approximation which gives rise to the Rayleigh–Onsager dissipation function[8] quadratic with respect to fluxes, and in this case the dissipation terms may be regarded as forming a "force field". In other words, the Rayleigh–Onsager dissipation function is a kind of potential function for a class of macroscopic processes, i.e., for linear transport processes near equilibrium.)

One of the purpose of the present paper is to study possible connections between the topography of an entropy production surface and trajectories that macroscopic processes can take in the space defined above. It turns out that in a case studied, it appears one can even predict qualitative shapes of the possible trajectories by simply inspecting the topography of the entropy production surface and the position of the initial condition on the surface if the stability of the steady states of the evolution equations is known. Evidence for this connection is not sufficiently broad as to let us formulate a set of definite rules at present, but it presents an intriguing possibility for some useful rules. In view of the necessity of numerical solution of the evolution equations in the case of nonlinear processes and its time-consuming nature, this kind of qualitative correlation, if there is a sufficient generality to it, can be extremely useful for model building for macroscopic phenomena. We show an example of a plausible correlation by performing calculations with a particular model constructed for current instability phenomena in semiconductors subject to an external electric field. Since Eq. (1.1) represents wide-ranging macroscopic phenomena in nature, we believe that the idea could be general and applicable to other processes covered by Eq. (1.1), although in another case studied the correlation is a little ambiguous and thus further studies are needed.

Our calculation of trajectories shows that the current can exhibit limit cycles when the field strength is larger than a critical value. This appearance of limit cycles seems to explain some current fluctuations[9] reasonably well. The entropy production associated with a limit cycle is shown to fluctuate rapidly. However, the average entropy production over a cycle is smaller than the value of the entropy production for the steady state that has just turned unstable and bifurcated into a limit cycle. This feature is demonstrated explicitly. This is similar to an observation made in connection with the gycolysis cycle[10,11] that if there is a limit cycle of a process in the system the entropy production over a cycle tends to be lower than otherwise. This appears to be an interesting observation which may have a significant implication. The fact that it is shown by two entirely different systems makes the observation more convincing.

In Sec. II we present a model for entropy production and corresponding evolution equations used for our study in this paper. The qualitative differences between the present and previous entropy production surfaces will be pointed out and discussed. In Sec. III steady states of the evolution equations and their stability will be discussed. In Sec. IV we consider approximate solutions for the evolution equations and in Sec. V are presented numerical solutions along with relevant quantities such as the current–voltage characteristic, the entropy production over a limit cycle, etc. Section VI is for discussion and conclusion.

II. ENTROPY PRODUCTION AND EVOLUTION EQUATIONS FOR FLUXES

In a previous paper[6] we studied dynamical evolutions of currents due to carriers of two different effective masses m_1^* and m_2^* in semiconductors subject to an external electric field. The study was based on a pair of phenomenologically assumed evolution equations for mass fluxes, which were made consistent with the second law of thermodynamics by requiring the dissipative terms in them to satisfy the condition (1.2). In the theory formulated, we approximated the entropy gradients $X_i^{(\alpha)}$ with a linear function of $\hat{\Phi}_i^{(\alpha)}$:

$$X_i^{(\alpha)} = -g_i^{(\alpha)}\hat{\Phi}_i^{(\alpha)}, \tag{2.1}$$

where in the case of mass fluxes, i.e., $\alpha = 4$,

$$g_i^{(\alpha)} = 1/c_i$$

where c_i denoting the mass density fraction ρ_i/ρ. With this approximation the entropy production was taken in the form

$$\begin{aligned}\sigma = T^{-1}[&L_{11}\hat{J}_1^2 + L_{22}\hat{J}_2^2 + (L_{12}+L_{21})\hat{J}_1\hat{J}_2 \\ &+ N_1\hat{J}_1^2(\lambda_1\hat{J}_1 + \lambda_2\hat{J}_2 - q_1)^2 \\ &+ N_2\hat{J}_2^2(\lambda_1\hat{J}_1 + \lambda_2\hat{J}_2 - q_2)^2],\end{aligned} \tag{2.2}$$

where L_{ij}, N_i, λ_i, and q_i $(i,j = 1,2)$ are taken as phenomenological parameters. As was shown in a previous paper,[6] the coefficients L_{ij} are related to the linear mobilities (transport coefficients) of the carriers and the nonlinear parameters N_i, λ_i, and q_i are related to nonlinear transport coefficients which may be traced, according to the kinetic theory of carriers,[1(d),4], to electron–electron collisions and higher order electron–phonon collision terms arising when, e.g., the Boltzmann collision integral is expanded in a series of fluxes. The nonlinear parameters do not appear in the theories that take linear thermodynamic force-flux relations as in the work by Landsberg and others.[12] The nonlinear contributions in effect reduce the mobility of carriers as the external field strength increases beyond a certain threshold value. This is shown in Ref. 6.

Substituting Eq. (2.1) into it and comparing the resulting equation with Eq. (2.2) for the diffusion flux part, i.e., for $\alpha = 4$, we find the dissipative term in the form

$$\Lambda_i^{(4)} = -\hat{L}_{ii}\hat{J}_i - \hat{L}_{ij}\hat{J}_j - \hat{N}_i\hat{J}_i(\lambda_1\hat{J}_1 + \lambda_2\hat{J}_2 - q_i)^2, \tag{2.3}$$

where

$$\hat{L}_{ij} = c_i L_{ij}, \quad \hat{N}_i = c_i N_i. \tag{2.4}$$

If the field is sufficiently strong, then the concentration gradient term is smaller than the electric field term in the thermodynamic force $X_i^{(4)}$;

$$\chi_i^{(4)} = -\operatorname{grad}_T \hat{\mu}_i + (z_i - z)\mathbf{E} + v\operatorname{grad} p.$$

When the concentation gradient terms are neglected and the assumptions are made that there are no heat fluxes and stress phenomena, the evolution equations for the mass flux densities $\hat{J}_1$ and $\hat{J}_2$ are as follows:

$$\rho \frac{d}{dt}\hat{J}_1 = \rho_1 z_1 \mathbf{E} + \Lambda_1^{(4)},$$
$$\rho \frac{d}{dt}\hat{J}_2 = \rho_2 z_2 \mathbf{E} + \Lambda_2^{(4)}. \tag{2.5}$$

We have assumed that there are only two independent mass fluxes to consider as a major contributing factor to the current. We remark that the mass flux of positively charged carriers is treated as the dependent flux by virtue of the relation

$$\sum_{i=1}^{r} \mathbf{J}_i = 0,$$

where r denotes the number of species. Dynamical solutions of Eq. (2.5) are studied in detail in the case of $X_i^{(4)}$ given by Eq. (2.3) in the previous paper[6] cited above.

The entropy production in Eq. (2.2) consists of two qualitatively distinctive parts: The first three terms on the right represent the entropy production due to the linear processes since they yield a set of linear evolution equations when the last two terms on the right, i.e., the nonlinear terms, are neglected. The last two terms give rise to nonlinear evolution equations and are responsible for various nonlinear phenomena associated with the current in semiconductors studied previously.[6] In the model we studied it was assumed that

$$q_1 = q_2 = q.$$

In that case the nonlinear part σ_{non} of the entropy production in Eq. (2.2):

$$\sigma_{\text{non}} = T^{-1}(N_1 \hat{J}_1^2 + N_2 \hat{J}_2^2)(\lambda_1 \hat{J}_1 + \lambda_2 \hat{J}_2 - q)^2$$

vanishes along the line L defined by the equation

$$\lambda_1 \hat{J}_1 + \lambda_2 \hat{J}_2 - q = 0. \tag{2.6}$$

As a consequence, the entropy production surface is folded along the line L and thus has two minima, one at the origin and along L, and one maximum along a line parallel to L and lying between the origin and L; see Fig. 1. This surface can give rise to trajectories going through a pitchfork bifurcation in the current–voltage characteristic. The trajectories, however, do not oscillate in the $(\hat{J}_1, \hat{J}_2)$ phase plane. There are two stable and one unstable steady state showing up as the field strength passes a critical value α_x, and the trajectory tends to either one of the two stable steady states, depending on the initial condition. The relatively simple geometric structure of the entropy production surface appears to rule out any unexpected complicated behavior of the trajectory. We will come back to this aspect of trajectories later on.

On the belief that the topography of the entropy production surface has much to do with the topology of the trajectories, we have introduced an additional feature in the entropy production surface in the following manner. The nonlinear part of the entropy production surface is modified such that there appears an additional locus of minima besides the line L defined by Eq. (2.6). The entropy production is thus assumed to take the form

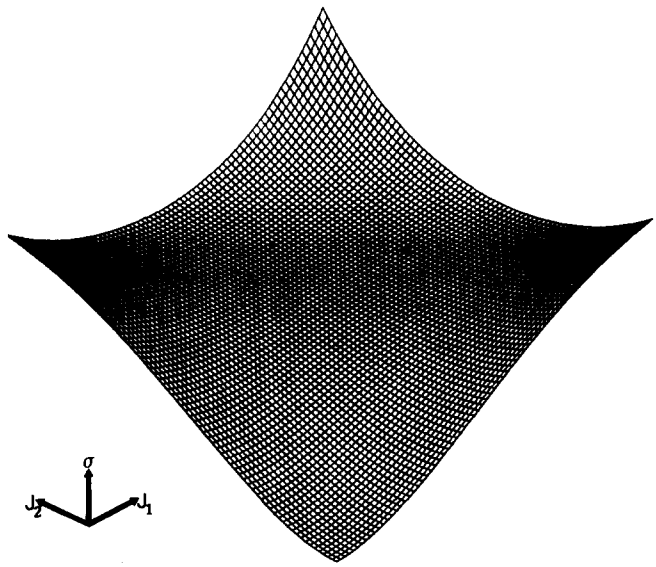

FIG. 1. The entropy production surface for the previous model. Its mathematical formula is given by Eq. (2.2).

$$\sigma = T^{-1}[L_{11}\hat{J}_1^2 + L_{22}\hat{J}_2^2 + (L_{12} + L_{21})\hat{J}_1\hat{J}_2 + \hat{a}(\hat{J}_1 - \hat{J}_2)^2(\lambda_1 \hat{J}_1 + \lambda_2 \hat{J}_2 - q)^2], \tag{2.7}$$

where $\hat{a}$ is a parameter characterizing the strength of the nonlinear term and $\alpha = \mathbf{E}\cdot\mathbf{E} = E^2$. The meanings of L_{ij} are the same as in Eq. (2.2); see also Eq. (3.3) below for their meanings. We remark that here we are not concerned as yet about a microscopic justification of the nonlinear term when we write σ as in Eq. (2.7). Instead, we are trying to see dynamical consequences of the particular form for σ postulated. The nonlinear part of σ has zeros along the two lines defined by

$$\lambda_1 \hat{J}_1 + \lambda_2 \hat{J}_2 - q = 0, \tag{2.8a}$$
$$\hat{J}_1 - \hat{J}_2 = 0, \tag{2.8b}$$

where the first line is exactly the same as line L and the second line is an additional feature. We will call them L_1 and L_2, respectively. Since the parameters in λ_1 and λ_2 are taken positive, line L_1 crosses line L_2 at $(\hat{J}_1, \hat{J}_2) = (\hat{J}_{1c}, \hat{J}_{2c})$, where

$$\hat{J}_{1c} = \hat{J}_{2c} = q(\lambda_1 + \lambda_2)^{-1}. \tag{2.9}$$

Therefore, the entropy production surface has two valleys crossing at $(\hat{J}_{1c}, \hat{J}_{2c})$ and ascending in the direction of increasing $\hat{J}_1$ and $\hat{J}_2$. Presented in Fig. 2 are the cross sections of the entropy production surface cut along a family of lines $J_1 = B - J_2$ determined by various values of B. Clearly, there is a ridge (a locus of maxima) between L_1 and L_2. The valleys are merged in the lower left corner in the phase space where $(\hat{J}_{1c}, \hat{J}_{2c})$ is located. Roughly speaking, the surface in the upper part looks like the exterior of a cone fitted with a trough on each side and the surface in the lower left corner looks like a section of the tip side interior of a cone sliced from its tip. In this conneciton see also Fig. 4(a) which contains isoentropy-production curves.

The dissipative terms corresponding to the entropy production surface (2.7) are obtained by using the same procedure as for Eq. (2.3):

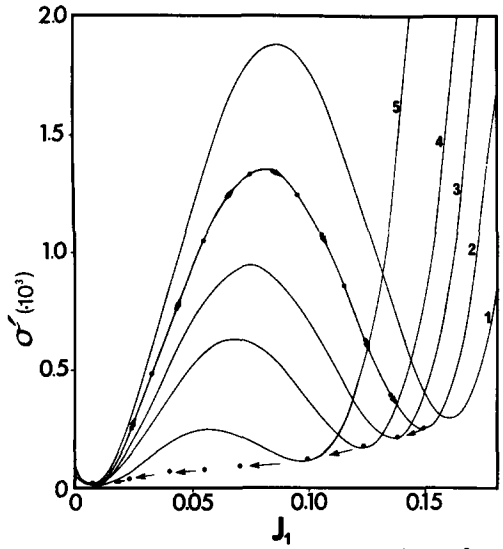

FIG. 2. Cross sections of the entropy production surface for the new model. The cut is along the line $J_1 = B - J_2$. The mathematical formula for the entropy production is given by Eq. (2.7). The arrows indicate a trajectory. The cross sections 1, 2, ..., 5 are, respectively, for $B = 0.324, 0.300, 0.275, 0.250, 0.200$. The values of α is 2.25.

$$\Lambda_1^{(4)} = -\hat{L}_{11}\hat{J}_1 - \hat{L}_{12}\hat{J}_2 - c_1\hat{a}(\hat{J}_1 - \hat{J}_2)(\lambda_1\hat{J}_1 + \lambda_2\hat{J}_2 - q)^2 , \tag{2.10}$$

$$\Lambda_2^{(4)} = -\hat{L}_{21}\hat{J}_1 - \hat{L}_{22}\hat{J}_2 + c_2\hat{a}(\hat{J}_1 - \hat{J}_2)(\lambda_1\hat{J}_1 + \lambda_2\hat{J}_2 - q)^2 .$$

When these dissipative terms are substituted into Eq. (2.5), there follow the evolution equations for $\hat{J}_1$ and $\hat{J}_2$ corresponding to the entropy production surface (2.7):

$$\frac{d}{dt}\hat{J}_1 = c_1 z_1 \mathbf{E} - \mathscr{L}_{11}\hat{J}_1 - \mathscr{L}_{12}\hat{J}_2 - a(\hat{J}_1 - \hat{J}_2)(\lambda_1\hat{J}_1 + \lambda_2\hat{J}_2 - q)^2 , \tag{2.11}$$

$$\frac{d}{dt}\hat{J}_2 = c_2 z_2 \mathbf{E} - \mathscr{L}_{21}\hat{J}_1 - \mathscr{L}_{22}\hat{J}_2 + a(\hat{J}_1 - \hat{J}_2)(\lambda_1\hat{J}_1 + \lambda_2\hat{J}_2 - q)^2 ,$$

where

$$\mathscr{L}_{ij} = \rho^{-1}\hat{L}_{ij} , \quad a = \rho^{-1}\hat{a}c_i . \tag{2.12}$$

We study these equations in what follows.

III. STEADY STATES AND THEIR STABILITY

To perform analysis of the evolution equations (2.11), we find it convenient to introduce mobilities $x(E,t)$ and $y(E,t)$ by the equations

$$\hat{J}_1 = c_1 z_1 x(E,t)\mathbf{E} , \qquad \hat{J}_2 = c_2 z_2 y(E,t)\mathbf{E} , \tag{3.1}$$

and transform Eq. (2.11) into evolution equations for $x(E,t)$ and $y(E,t)$. We assume that the density is constant with respect to time (adiabatic approximation) and that

$$\lambda_1 = \mathbf{E}/\hat{J}_{10} , \quad \lambda_2 = \mathbf{E}/\hat{J}_{20} ,$$

where $(\hat{J}_{10}, \hat{J}_{20})$ stands for the steady state defined by

$$\hat{J}_{10} = c_1 z_1 x_0 \mathbf{E} , \qquad \hat{J}_{20} = c_2 z_2 y_0 \mathbf{E} , \tag{3.2}$$

with x_0 and y_0 given by

$$x_0 = [\mathscr{L}_{22} - Z_{21}\mathscr{L}_{12} + \alpha a(1 + Z_{21})(2 - C)^2]/\Delta , \tag{3.3a}$$

$$y_0 = [\mathscr{L}_{11} - Z_{12}\mathscr{L}_{21} + \alpha a(1 + Z_{12})(2 - C)^2]/\Delta , \tag{3.3b}$$

$$\Delta = \mathscr{L}_{11}\mathscr{L}_{22} - \mathscr{L}_{12}\mathscr{L}_{21} + \alpha a(\mathscr{L}_{11} + \mathscr{L}_{22} + 2\mathscr{L}_{12})(2 - C)^2 , \tag{3.3c}$$

$$Z_{21} = 1/Z_{12} = c_2 z_2 / c_1 z_1 , \tag{3.3d}$$

$$q = C\mathbf{E} . \tag{3.3e}$$

Therefore, x_0 and y_0 may be regarded as the steady state mobilities of the charged carriers. The limiting zero-field mobilities are determined by phenomenological parameters (transport coefficients) $\mathscr{L}_{11}$, $\mathscr{L}_{22}$, $\mathscr{L}_{12} = \mathscr{L}_{21}$. Then the evolution equations for x and y takes the form

$$\frac{dx}{dt} = 1 - \mathscr{L}_{11}x - Z_{21}\mathscr{L}_{12}y - \alpha a(x - Z_{21}y)(x/x_0 + y/y_0 - C)^2 , \tag{3.4}$$

$$\frac{dy}{dt} = 1 - Z_{12}\mathscr{L}_{21}x - \mathscr{L}_{22}y + Z_{12}\alpha a(x - Z_{21}y)(x/x_0 + y/y_0 - C)^2 . \tag{3.5}$$

It is convenient to change the variables still further by writing

$$x = x_0 + u_1 , \qquad y = y_0 + u_2 .$$

Since

$$1 - \mathscr{L}_{11}x_0 - Z_{21}\mathscr{L}_{12}y_0 - \alpha a(x_0 - Z_{21}y_0)(2 - C)^2 = 0 , \tag{3.3'}$$

$$1 - Z_{12}\mathscr{L}_{21}x_0 - \mathscr{L}_{22}y_0 + Z_{12}\alpha a(x_0 - Z_{21}y_0)(2 - C)^2 = 0 ,$$

we easily find the evolution equations for u_1 and u_2:

$$\frac{du_1}{dt} = \lambda_{11}u_1 + \lambda_{12}u_2 - \alpha a Q(u_1,u_2) , \qquad \frac{du_2}{dt} = \lambda_{21}u_1 + \lambda_{22}u_2 + \alpha a Z_{12} Q(u_1,u_2) , \tag{3.6}$$

where

$$\lambda_{11} = -\mathscr{L}_{11} - \alpha a(2 - C)^2 - 2\alpha a(2 - C)(1 - Z_{21}y_0/x_0) , \tag{3.7a}$$

$$\lambda_{22} = -\mathscr{L}_{22} - \alpha a(2 - C)^2 + 2\alpha a Z_{12}(2 - C)(x_0/y_0)(1 - Z_{21}y_0/x_0) , \tag{3.7b}$$

$$\lambda_{12} = -Z_{21}[\mathscr{L}_{12} - \alpha a(2 - C)^2] - 2\alpha a(x_0/y_0)(1 - Z_{21}y_0/x_0)(2 - C) , \tag{3.7c}$$

$$\lambda_{21} = -Z_{12}[\mathscr{L}_{21} - \alpha a(2-C)^2] + 2\alpha a Z_{12}(2-C)(1 - Z_{21}y_0/x_0)\,, \tag{3.7d}$$

$$Q = 2(2-C)(u_1 - Z_{21}u_2)(u_1/x_0 + u_2/y_0) + (x_0 - Z_{21}y_0 + u_1 - Z_{21}u_2(u_1/x_0 + u_2/y_0)^2\,. \tag{3.7e}$$

Equation (3.6) can be used for investigating steady states for the system. We find that there are no other steady states than (x_0, y_0), i.e., $(u_1,u_2) = (0,0)$. This is shown in Appendix A.

We now perform stability analysis of the physical steady state (0,0) just mentioned. The eigenvalues are given by

$$\omega^{(\pm)} = \tfrac{1}{2}(\lambda_{11} + \lambda_{22}) \pm \tfrac{1}{2}[(\lambda_{11} - \lambda_{22})^2 + 4\lambda_{12}\lambda_{21}]^{1/2}\,. \tag{3.8}$$

We find that the real parts of the eigenvalues change the sign from negative to positive as α crosses the critical value α_c which is determined by the equation

$$\lambda_{11}(\alpha) + \lambda_{22}(\alpha) = 0\,. \tag{3.9}$$

For the parameter set chosen for this work, the critical value α_c is

$$\alpha_c \cong 2.19$$

corresponding to the critical value of E at $E_c = 1.48$. As will be shown, for $\alpha \geqslant \alpha_c$ the steady state turns unstable and bifurcates into a limit cycle. Since the steady state is stable for $\alpha < \alpha_c$, the current–voltage characteristic can be calculated with the steady state fluxes up to the critical point. After the critical point there does not exist a steady current, but an oscillating current shows up which fluctuates between the maximum and minimum determined by the field strength as will be shown in Sec. V.

IV. APPROXIMATE SOLUTIONS OF THE EVOLUTION EQUATIONS

The general solution of the evolution equations appears to be impossible to obtain by an analytic means. However, it is still possible to obtain approximate analytic solutions if the polar coordinates are used. Although it is not possible to use them to draw a general, precise conclusion on the dynamic behavior of the system based on the approximate solutions, they serve a useful function of assuring us that the numerical solutions to be discussed in the next section are indeed reliable. We discuss them below.

Let us write the variables u_1 and u_2 in polar coordinates (r,θ):

$$u_1 = r\cos\theta\,, \qquad u_2 = r\sin\theta\,. \tag{4.1}$$

Then we obtain from Eq. (3.6) the following radial and angular equations:

$$\frac{d}{dt}\ln r = f_1(\theta) - \alpha a(\cos\theta - Z_{12}\sin\theta)Q_r(r,\theta)\,, \qquad \frac{d\theta}{dt} = f_2(\theta) + \alpha a(Z_{12}\cos\theta + \sin\theta)Q_r(r,\theta)\,, \tag{4.2}$$

where

$$f_1(\theta) = \lambda_{11}\cos^2\theta + \lambda_{22}\sin^2\theta + (\lambda_{12} + \lambda_{21})\cos\theta\sin\theta\,, \tag{4.3a}$$

$$f_2(\theta) = \lambda_{21}\cos^2\theta - \lambda_{12}\sin^2\theta + (\lambda_{22} - \lambda_{11})\cos\theta\sin\theta\,, \tag{4.3b}$$

$$Q_r(r,\theta) = Q(r,\theta)/r\,. \tag{4.3c}$$

These equations are easily generated by starting with the relations

$$r^2 = u_1^2 + u_2^2\,, \quad \tan\theta = u_2/u_1\,,$$

and differentiating them and using Eq. (3.6). $Q_r(r,\theta)$ is obviously a nonlinear function of r and θ. By dividing the first equation in Eq. (4.2) with the second, we obtain the orbit equation

$$\frac{d\ln r}{d\theta} = [\,f_1(\theta) - \alpha a(\cos\theta - Z_{12}\sin\theta)Q_r\,] \,/\, [\,f_2(\theta) + \alpha a(Z_{12}\cos\theta + \sin\theta)Q_r\,]\,. \tag{4.4}$$

This equation is not integrable analytically, but we can obtain approximate analytic solutions which supply a reasonably good notion of the solution. Since Q_r is a quadratic function of r, as r increases to a sufficiently large value Eq. (4.4) approximately takes the form

$$\frac{d\ln r}{d\theta} \cong -\frac{\cos\theta - Z_{12}\sin\theta}{Z_{12}\cos\theta + \sin\theta}\,. \tag{4.5}$$

This equation may be easily integrated to yield

$$r = r_0(Z_{12}\cos\theta + \sin\theta)^{-1}\,, \tag{4.6}$$

where r_0 is the value of r at $\theta = 0$. It is a periodic function of θ. Note that this may be written as

$$Z_{12}u_1 + u_2 = r_0 \tag{4.6'}$$

indicating that it is a line of a negative slope in the (u_1,u_2) plane. In fact, it is a family of lines with a negative slope.

If the radius is sufficiently small, then Eq. (4.4) may be written approximately as

$$\frac{d\ln r}{d\theta} \cong \frac{f_1(\theta)}{f_2(\theta)}\,. \tag{4.7}$$

Terms of $O(r)$ are neglected on the right-hand side. It is reasonable to do so if r is sufficiently small. Reorganizing the right-hand side of Eq. (4.7), we may write the differential equation in the form

$$\frac{d\ln r}{d\theta} = \frac{\lambda_{11} + \lambda_{22} + (\lambda_{12} + \lambda_{21})\sin 2\theta - (\lambda_{22} - \lambda_{11})\cos 2\theta}{\lambda_{21} - \lambda_{12} + (\lambda_{12} + \lambda_{21})\cos 2\theta + (\lambda_{22} - \lambda_{11})\sin 2\theta}\,. \tag{4.7'}$$

This equation is also easily integrable.[13] Since $(\lambda_{11} - \lambda_{22})^2 + 4\lambda_{12}\lambda_{21} < 0$ for the steady state (x_0,y_0), we obtain the orbit in the form

$$\ln\{Cr[\lambda_{21}-\lambda_{12}+(\lambda_{22}-\lambda_{11})\sin 2\theta+(\lambda_{12}+\lambda_{21})\cos 2\theta]^{1/2}\}$$
$$=\frac{(\lambda_{11}+\lambda_{22})}{2|(\lambda_{11}-\lambda_{22})^2+4\lambda_{21}\lambda_{12}|^{1/2}}\tan^{-1}\left(\frac{\lambda_{22}-\lambda_{11}-2\lambda_{12}\tan\theta}{|(\lambda_{22}-\lambda_{11})^2+4\lambda_{12}\lambda_{21}|^{1/2}}\right), \tag{4.8}$$

where C is the integration constant. This solution shows that the trajectory is periodic, but it does not necessarily imply that the exact solution is a limit cycle. However, the numerical solutions indicate that the solution is indeed a limit cycle.

V. TRAJECTORIES AND THE ENTROPY PRODUCTION SURFACE

A. Trajectories

The evolution equations (3.4) are solved numerically by employing an integration routine. In order to ascertain that the steady state solution in the domain of $\alpha<\alpha_c$ is indeed attained in a sufficiently long time span, we have numerically solved Eq. (3.4) at a few points in the domain. The solutions, irrespective of the initial conditions chosen, rather quickly approach the steady state (x_0,y_0) as expected. Since there is nothing very interesting happening in the domain of $\alpha<\alpha_c$, we shall not dwell on it much. The subsequent discussions will be devoted almost entirely to the dynamical behavior of the system in the more interesting domain of $\alpha\geqslant\alpha_c$. The parameters of the equations chosen for the calculation are summarized in Table II.

The steady state (x_0,y_0), or equivalently $(u_1,u_2)=(0,0)$, turns unstable as α_c is crossed from below and the solution bifurcates into a limit cycle as suggested by the approximate orbit obtained in the previous section. An example for such a limit cycle at $\alpha=2.25$ is given in Fig. 3. It is a stable cycle independent of the initial conditions taken. The two curves tending to the limit cycle in Fig. 3 represent the trajectories starting from two different initial conditions. Similar calculations were performed at many different points in $\alpha>\alpha_c$, and there invariably appears a limit cycle at each point, but the size of the limit cycle gets smaller as α increases. In Figs. 4(a) and 4(b) presented are the trajectories (limit cycles) superimposed on the isoentropy-production curves in order to see which part of the entropy production surface is explored by the limit cycle. The dots in Figs. 4(a) and 4(b) represent the trajectory points and we have presented only a part of the limit cycle in the case of Fig. 4(b). The broken lines in the figures denote the lines L_1 and L_2 along which the nonlinear part of the entropy production vanishes; see Eq. (2.3). The valleys in the entropy production surface are either almost superimposed on the broken lines or almost parallel to them. Clearly, the trajectories move along the minima of the valleys most of the time. In order to show this feature from another vantage point, we cut the entropy production surface with the asymptotic trajectory line defined by Eq. (4.6') which may be put in the form

TABLE II. Parameters.

$\mathscr{L}_{11}=1.10\times10^{-2}\ \mathrm{s}^{-1}$
$\mathscr{L}_{22}=1.70\times10^{-4}\ \mathrm{s}^{-1}$
$\mathscr{L}_{12}=-1.48\times10^{-5}\ \mathrm{s}^{-1}$
$\mathscr{L}_{21}=\mathscr{L}_{12}$
$a=3.10\times10^{-4}\ \mathrm{m}^2\ \mathrm{s}^{-1}\ \mathrm{V}^{-2}$
$Z_1=n_1e_1=4.54\times10^{-5}\ \mathrm{C\ m}^{-3}$
$Z_{12}=1.05$
$C=1.81$

$$\mathbf{J}_2=B-\mathbf{J}_1, \tag{5.1}$$

where B is a parameter varied to cut the surface, and plot the cross section of the entropy production surface thus generated. They are given in Fig. 2 where the arrows indicate roughly the trajectory followed by the system in the case of $\alpha=2.25$ corresponding to the trajectory in Fig. 4(a). Since the valley on the left is rather flat, there is an accumulation of the cross section curves, but the curves are, when viewed along the J_2 axis, spread out upward along the J_2 axis. The figure shows that, when projected onto the line defined by Eq. (5.1), the problem becomes that of a dynamical system with a bistability. In the present case the system is not oscillating back and forth between the two minima, but makes a roundabout detour along the valleys to revisit the minima repeatedly.

B. Current-voltage characteristic

The total current may be calculated by using the steady state formulas (3.3a) and (3.3b) and the numerical solutions in the domain $\alpha\geqslant\alpha_c$. It is defined by

$$\mathbf{J}=\rho(\hat{J}_1+\hat{J}_2)=\rho(c_1z_1x+c_2z_2y)\mathbf{E}, \tag{5.2}$$

where the time is taken sufficiently long so that the current

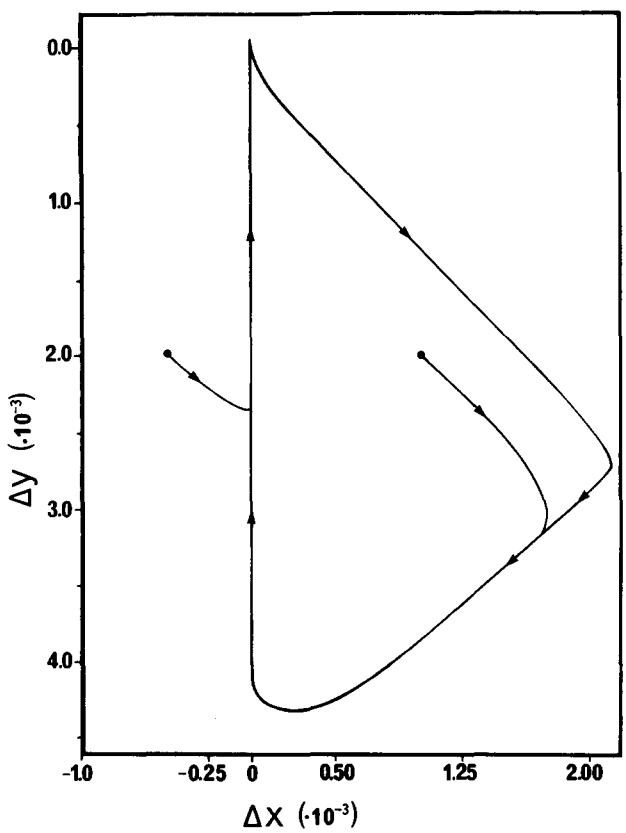

FIG. 3. An orbit in the (x,y) plane. Note that x and y are the mobilities of the two carriers. The orbit is a stable limit cycle. $\alpha=2.25$. $\Delta x=x-x_0$ and $\Delta y=y-y_0$.

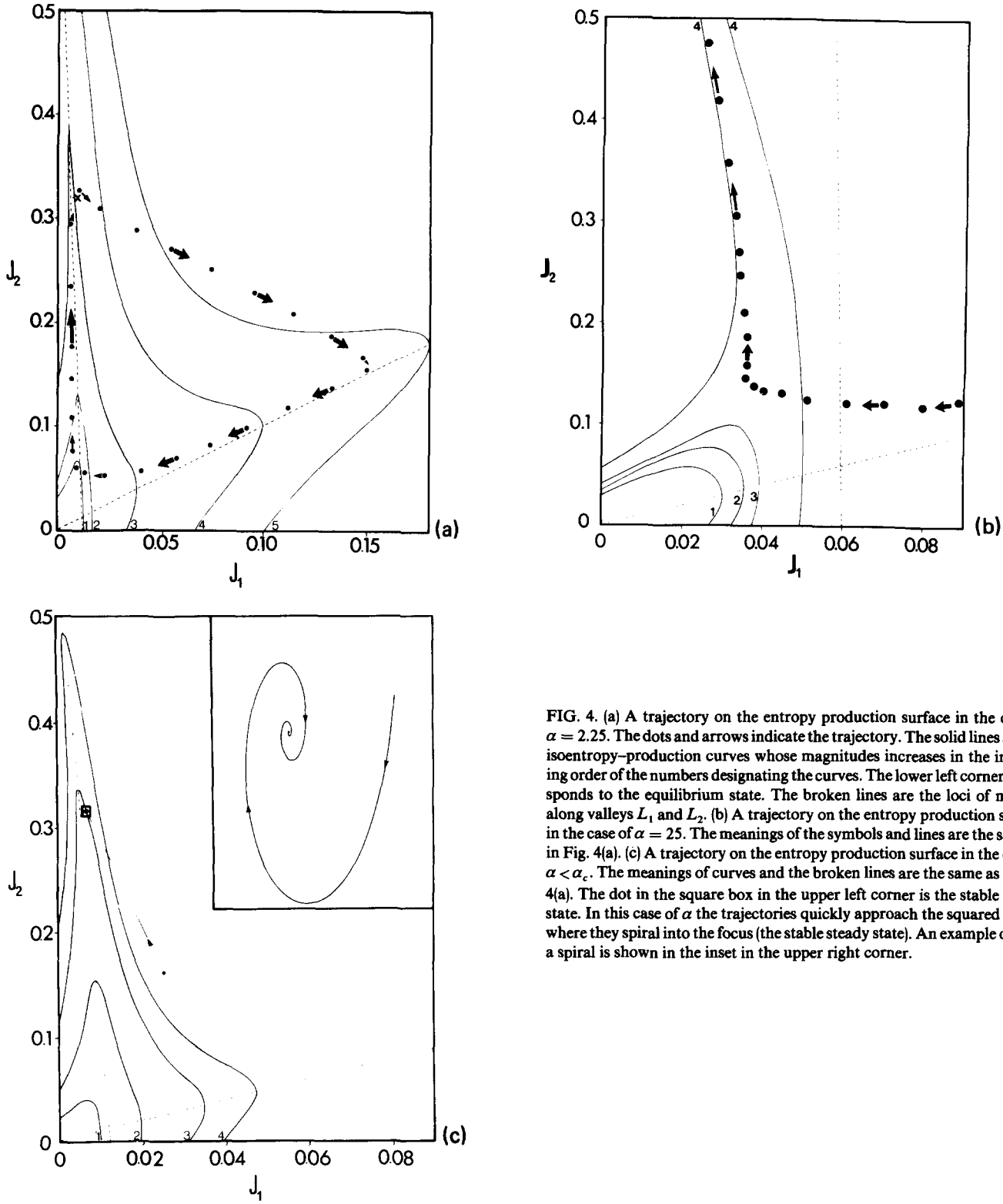

FIG. 4. (a) A trajectory on the entropy production surface in the case of $\alpha = 2.25$. The dots and arrows indicate the trajectory. The solid lines are the isoentropy–production curves whose magnitudes increases in the increasing order of the numbers designating the curves. The lower left corner corresponds to the equilibrium state. The broken lines are the loci of minima along valleys L_1 and L_2. (b) A trajectory on the entropy production surface in the case of $\alpha = 25$. The meanings of the symbols and lines are the same as in Fig. 4(a). (c) A trajectory on the entropy production surface in the case of $\alpha < \alpha_c$. The meanings of curves and the broken lines are the same as in Fig. 4(a). The dot in the square box in the upper left corner is the stable steady state. In this case of α the trajectories quickly approach the squared region where they spiral into the focus (the stable steady state). An example of such a spiral is shown in the inset in the upper right corner.

becomes steady in the case of $\alpha < \alpha_c$ or independent of the initial conditions in the case of limit cycles in the domain $\alpha \geqslant \alpha_c$. The current vs $E = |\mathbf{E}|$ is plotted in Fig. 5 where the minimum and maximum values of the current are indicated by horizontal bars for the oscillating currents, along with the current values (the dots) corresponding to the center of the limit cycles. In the low voltage region the Ohmic law is obeyed, but the current gradually deviates from the prediction by the linear law as the voltage increases, eventually turning into an oscillating current. The frequency ω of oscillation also depends on the field strength and decreases by an order of magnitude over a small span of voltage before it starts increasing gradually again. The field dependence of frequency is given in Fig. 6. In the previous model for the Gunn effect the fluctuations in current appeared as a consequence of fluctuating initial conditions coupled with a pitch-

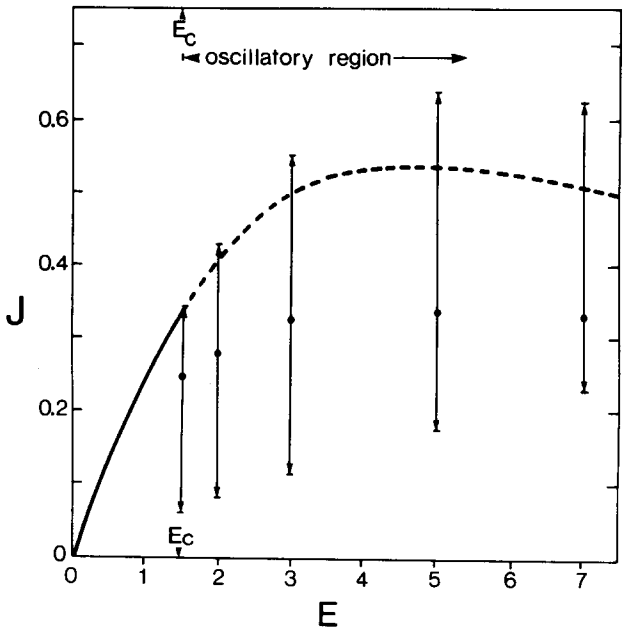

FIG. 5. Current–bias voltage characteristic. The broken line is the locus of the unstable steady state and the lines with arrows indicate the amplitudes of oscillation by the limit cycles at different values of the field strength.

fork bifurcation. In the present model we have genuine oscillations completely independent of initial conditions and inherent to the system itself. We believe that the present model may be applied to study some current oscillation phenomena in semiconductors. We reserve it for a subsequent study.

C. Entropy production and limit cycles

When close examination is made of the trajectories described by the limit cycles superimposed on the isoentropy-production map, they reveal that the entropy production wildly fluctuates, and a trajectory moves from high entropy production states to low entropy production states. This raises a question as to the net entropy production over a cycle. Since irreversibility is intimately tied up with the entropy production and the dynamic evolution of a process is *tightly constrained* to the second law restriction in the present theory, it is of importance to study the behavior of the entropy production. We carry out a study on the question.

We have calculated the temporal evolution of the entropy production corresponding to the limit cycles. The entropy productions are calculated by using Eq. (2.7) and the numerical solutions of Eq. (3.4) over several periods of oscillation. In Fig. 7 is shown the entropy production over two periods of oscillation for the limit cycle at $\alpha = 2.25$. This limit cycle is also used in the previous figures. The ordinate is the entropy production relative to that (σ_0) of the steady state (x_0, y_0) which has turned unstable in the domain $\alpha \geqslant \alpha_c$. We will denote this entropy production difference by $\Delta\sigma = \sigma - \sigma_0$. It is a sharply peaked function with the peak position corresponding to the maximum in one of the curves in Fig. 2 and equivalently to the ridge roughly lying along the diagonal in Fig. 4(a). The lowest value of $\Delta\sigma$ corresponds to the lower left-hand corner of the limit cycle. The left-hand side of the peaks corresponds to the trajectory from the upper left-hand corner to roughly the midpoint on the way to the right-hand corner; Figs. 2 and 3. This path takes a short, but a sizable burst of energy for the system to traverse it. Nevertheless, the system ends up dissipating less energy over a period of the cycle, compared with what it would if it remained at the unstable steady state from which the limit cycle has bifurcated. In order to show this, we calculate the average entropy production over a period by using the formula

$$\overline{\Delta\sigma} = T^{-1}\rho\tau^{-1}\int_0^{\tau} dt\,\Delta\sigma(t)\,, \tag{5.3}$$

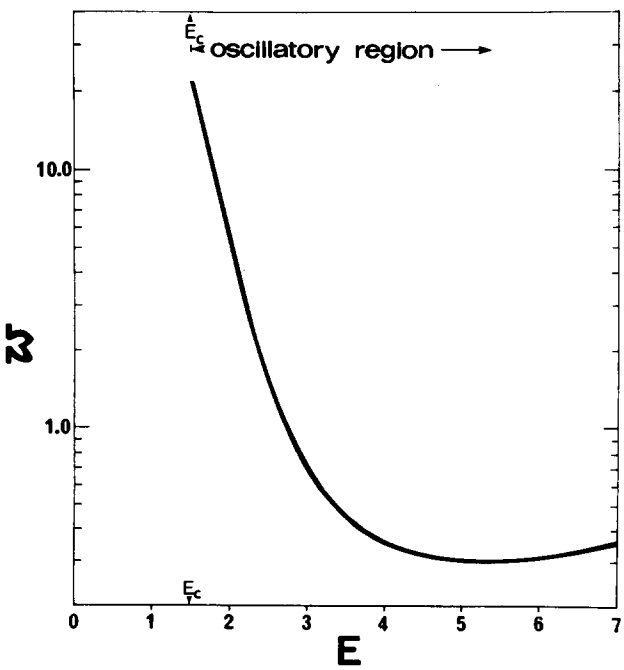

FIG. 6. The oscillation frequency vs field strength.

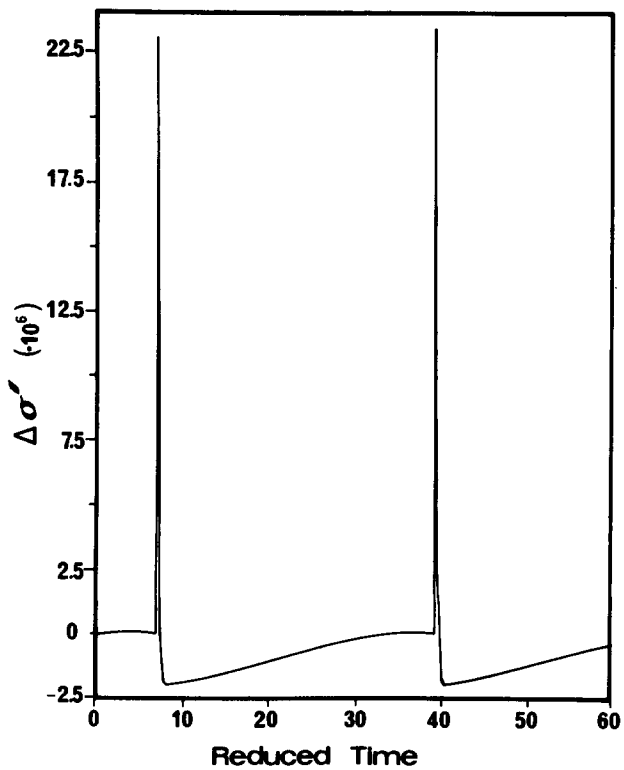

FIG. 7. The entropy production vs time in the case of a limit cycle.

where τ is the period. Presented in Fig. 8 is $\overline{\Delta\sigma}$ computed for a few values of E. As is clear from the figure, the entropy production is, on the average, smaller than that of the unstable steady state (x_0, y_0), and it decreases with the increasing field strength. That is,

$$\overline{\Delta\sigma} \leqslant 0 \quad \text{or} \quad \bar{\sigma} \leqslant \sigma_0 \tag{5.3'}$$

over a limit cycle. This appears to replace the minimum entropy production theorem in linear irreversible thermodynamics. A similar phenomenon was observed by Ross and his co-workers[10,11] in connection with the glycolysis cycle, although they have computed the entropy production somewhat differently by using a version essentially equivalent to a linearized form of Eq. (5.3). It appears that this could be a universal phenomenon characteristic of limit cycles. Implication of such entropy production reduction by a limit cycle could be far reaching in understanding diverse natural phenomena involving macroscopic oscillations.

We remark that $\Delta\sigma(t)$ changes continuously, although rather abruptly, from the base line, i.e., $\Delta\sigma(t) = 0$, over a cycle and the apparent sudden drop in its average value $\overline{\Delta\sigma}$ at $E = E_c$ is a manifestation of a significant reduction in the average entropy production when the dimension of the steady state changes from zero (a focus) to one (a closed curve) as the threshold value of E is crossed, i.e., when there appears a limit cycle which spends a major portion of the period in the low entropy production states dissipating less energy.

Once we clearly understand the topography of the entropy production surface and the steady state structure of the evolution equations, it is possible to comprehend the trajectories which are constrained to move on the entropy production surface. In order to elaborate on this aspect of our study, we first make the following observation. The phenomenological coefficients in the evolution equations (3.4) are a measure[1(d),4] of interactions of the carriers with other carriers and phonons, although the precise modes of interaction are not apparent and neither are they a main concern of a phenomenological theory. In any event, since the external field

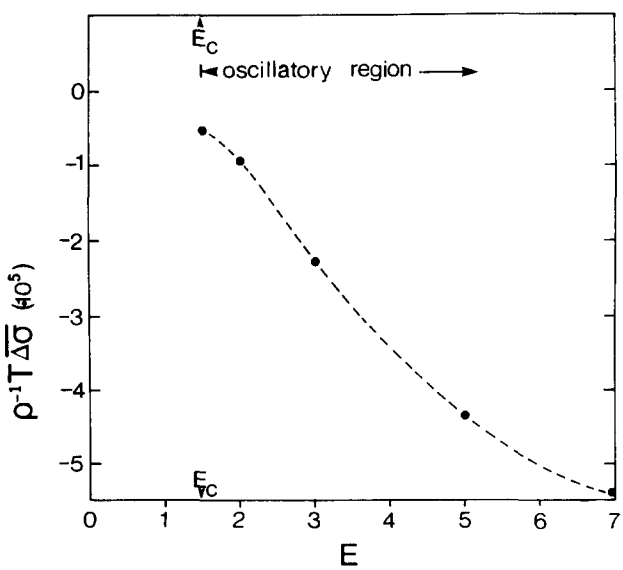

FIG. 8. Average decrease in the entropy production vs field strength in the case of limit cycles.

continuously accelerates the carriers, the latter move faster and as they get accelerated, their energy is dissipated due to their interactions with phonons and other carriers. The unstable steady state at $\alpha = 2.25$ appears at the upper left-hand corner of the limit cycle and is denoted by $\times$. As the slower species of the two carriers gains speeds due to its interaction and at the expense of the faster species and the external field, the system has no alternative but to dissipate energy by going over the hump to the L_2 valley, since that option is available and the only one available under the circumstances. Once the system gets to the right corner and then to the lower left corner of the limit cycle (trajectory), it has dissipated its energy and both species have lost their speed, yet with the help of the external field one species gradually gains the speed to bring the state of the system back up to the vicinity of the unstable steady state ($\times$); see Fig. 4(a). The whole process then repeats. This process of cycle would not have been realized if there were not the second valley or if there were a stable steady state in the energetically accessible region in the entropy production surface. Therefore, we see that at least in the case of the present model the topography of the entropy production surface and a knowledge of the steady states of the evolution equations and their stability would even enable us to predict the qualitative topological property of the trajectory. This picture gets sharpened if we look at the behavior of the trajectory in the case of $\alpha < \alpha_c$. In this case the steady state acts as an attractor to which the trajectories quickly approach no matter where the initial conditions are located on the entropy production surface; see Fig. 4(c). Unfortunately, the picture gets a little blurred when we examine the trajectories for the model[6] taken previously for a current fluctuation phenomenon in the Gunn oscillator for which the entropy production is given by Eq. (2.2). In the latter case the entropy production surface shows a valley (L_3) starting from the equilibrium state (i.e., the origin) along the line $\mathbf{J}_2 = Z_{12}\mathbf{J}_1$ which meets another valley (L_1) away from the origin and almost perpendicularly to the former. The valley structure therefore has a T shape. Steady state analysis shows that the minima of the L_3 valley are on the locus of the steady state flanked by two stable steady states on the locus. Since the topography of the entropy production surface is much simpler in structure in the latter case, this does not provide a possible mechanism for an oscillatory motion, and there are two stable steady states at a given value of α to which the trajectory can tend, the trajectory is relatively simple and at most a spiral converging to a focus. The trajectories do not tend to (x_g, y_g), i.e., (J_{1g}, J_{2g}), since it is unstable and thus a repeller. However, it turns out that predicting which way the trajectories will go by just inspecting the position of the initial condition on the entropy production surface is not as straightforward as in the case of the former model. As shown in Fig. 9, the initial conditions are roughly divided by a boundary passing through the unstable steady state into upper and lower subsets, the upper subset of initial conditions draining into the upper steady state while the lower subset draining into the lower stable state. However, we are unfortunately not able to associate the boundary of the subsets, in a clear cut manner, with a particular feature of the entropy production surface, although the upper part of

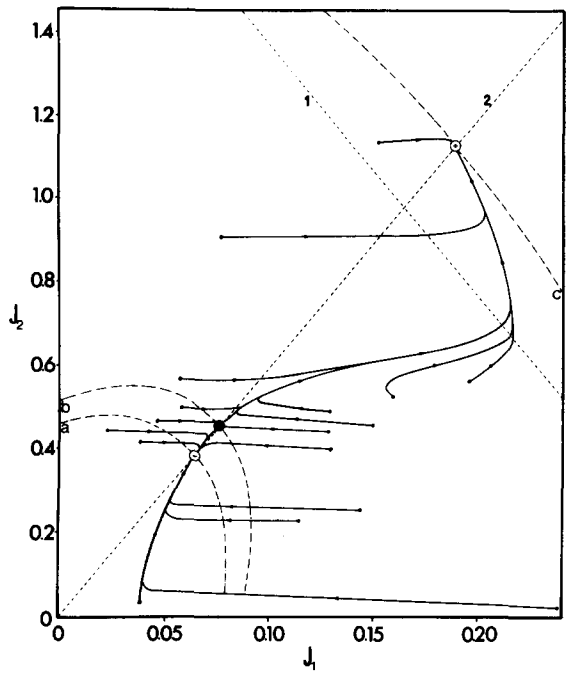

FIG. 9. The trajectories on the entropy production surface given by Eq. (2.2)—the old model. The filled circle denotes the unstable steady state and the open circle with + or − in it denotes the stable steady state. The broken lines are respectively defined by Eq. (2.6) and $J_1 = J_2$. It is noticeable that the initial conditions are divided into two distinctive subsets which tend to either of the upper and lower stable steady states. The boundary of the subsets are not clear at present. The dash–dot curves are the isoentropy-production curves corresponding to the steady states.

the surface has a more distinctive valley than does the lower part which is in fact tilted toward the origin and has a barely noticeable valley. In this sense, we could still correlate the trajectories with the entropy production surface structure, but it will be necessary to make further studies with entropy production surfaces with sharper distinguishing features in them.

All this argumentation is of course retrospective, but since it might guide us in future studies on nonlinear dynamics, we make the following conjecture with the evidence in hand, although narrow: *Given an entropy production surface and the steady states associated with the entropy production and their stability, it is possible to qualitatiely and roughly predict possible trajectories followed by a two-process system, without solving the evolution equations explicitly.* This conjecture is, of course, empirically obtained and is yet to be further substantiated. At least, it seems to give us a guide in numerical solutions of the evolution equations. In fact, we have often benefitted by this conjecture while performing numerical solutions, since it has helped us detect incorrect trajectories arising from numerical errors. It is probably possible to remove the word two-process from the conjecture and make it more general so that it can cover multiprocess sytems. We have not yet studied such a system to support the removal, but a difficulty with such study is that it is not easy to visualize a hypersurface for the entropy production required for such a system. Nevertheless, the generalization of the conjecture presents an intriguing possibility for studying complex macroscopic evolutions in nature in a systematic manner instead of using *ad hoc* procedures employed to construct evolution equations as is presently done in nonlinear dynamical studies.

Entropy production was proposed as a kind of Lyapounov function used in nonlinear analysis especially in connection with stability[15] of thermodynamic systems. The present study shows that it is not quite a Lyapounov function, although there are some tempting features in it that would appear to make it qualify as a Lyapounov function. The entropy production for linear dissipative processes—processes that can be described by linear approximations to the dissipative terms $\Lambda_i^{(\alpha)}$—can be regarded as a Lyapounov function, since it is a quadratic, and homogeneous, function of fluxes and thus has all the required properties for a Lyapounov function, but linear processes do not have features intrinsic to nonlinear processes and therefore are not so terribly interesting from the dynamical viewpoint; their dynamics are rather simple. The point we emphasize here as was done repeatedly before in different contexts[1,4–7] is that the entropy production is the seat of irreversibility and is intimately tied up with macroscopic dynamics, since the dissipative terms in the evolution equations are also closely related to the entropy production. One of the main tasks in irreversible thermodynamics is therefore in studying the role played by the entropy production for the process under consideration. This work with some numerical evidence represents an effort in that direction.

VI. DISCUSSION AND CONCLUSION

Since the entropy production is constrained to satisfy the second law of thermodynamics on one hand and gives the dissipative terms in the evolution equation on the other, we have further investigated some consequences of the notion that there should be some useful correlations between the entropy production and the macroscopic dynamic evolution of the system, which we might exploit in studying macroscopic phenomena. As a byproduct of this effort, we have found a pair of evolution equations which can give rise to limit cycles as the electric field strength passes through a critical value. This model opens up a new avenue of approach to the current fluctuation phenomena in semiconductors such as GaAs and will be studied in the future in connection with experimental data. In view of the fact that there are stable oscillatory phenomena[9] observed in semiconductors (e.g., GaAs), finding a set of equations yielding limit cycles is interesting and useful by itself, and the fact that it is an outcome of a particular feature in the entropy production surface is quite intriguing. It is something very difficult to dismiss as an oddity with little implication.

Another interesting finding we have made is the average entropy production over a limit cycle which tends to be decreased when compared with the entropy production corresponding to the stable steady state from which the limit cycle has just bifurcated. Confirming a similar observation made by Ross and his co-workers[10,11] on an entirely different system gives us the impression that it could be a wide-spread feature among systems exhibiting one or more limit cycles.

The emergence of a limit cycle in current has another significant implication in the theory of irreversible thermodynamics on which the present theory is based. In the pres-

ent theory the entropy change is given by the extended Gibbs relation[1] (1.3) and for a field-free case by the equation

$$Td\mathscr{S} = d\mathscr{E} + pdv - \sum_i \hat{\mu}_i dc_i + \sum_{i\alpha} X_i^{(\alpha)} \odot d\hat{\Phi}_i^{(\alpha)}, \quad (6.1)$$

where $\hat{\mu}_i$ is the chemical potential per unit mass of i. If there exists a stable steady state solution of the evolution equations and the solution relaxes to the steady state on a time scale shorter than the hydrodynamic relaxation time on which the conserved variables relax, the last term in Eq. (6.1) vanishes faster than the rest of the terms on the right-hand side of Eq. (6.1) and consequently the extended Gibbs relation tends to the local equilibrium Gibbs relation on the same time scale as the time taken by the fluxes to relax to their steady state value. In such situations the local equilibrium hypothesis[14–16] for the entropy change is sufficient, if we are interested in the entropy change on the hydrodynamic scale. However, the emergence of a limit cycle changes the situation since the fluxes are no longer steady and the entropy fluctuates periodically. Therefore, the local equilibrium hypothesis breaks down and the theory of irreversible thermodynamics on which our study here is based provides a way of handling such an extension. We remark that the theory has kinetic theory foundations as shown in previous papers.[1,4]

The conjecture proposed here for a possible correlation between the entropy production surface and trajectories requires further studies, but we have found it useful in studying macroscopic dynamics reported here. The present study seems to reinforce the notion that the entropy production as an expression for the second law not only holds an important key to understanding macroscopic phenomena, but also can be used for implementing study of macroscopic dynamical evolutions besides the second law constraints it imposes on the latter.

APPENDIX A: STEADY STATE

The steady state of Eq. (3.4), or equivalently Eq. (3.6), is determined by the pair of algebraic equations

$$\lambda_{11}u_1 + \lambda_{12}u_2 - \alpha a Q(u_1,u_2) = 0, \quad (A1)$$

$$\lambda_{21}u_1 + \lambda_{22}u_2 + Z_{12}\alpha a Q(u_1,u_2) = 0,$$

where the notations are defined in Eqs. (3.7a)–(3.7e). It is convenient for solving these equations to change the variables as follows:

$$\eta = \tfrac{1}{2}(u_1 + Z_{21}u_2), \quad (A2)$$

$$\xi = \tfrac{1}{2}(u_1 - Z_{21}u_2).$$

Then with the definitions of the following coefficients:

$$A^{(\pm)} = \tfrac{1}{2}[\lambda_{11} + Z_{21}\lambda_{21} \pm Z_{12}(\lambda_{12} + Z_{21}\lambda_{22})], \quad (A3)$$

$$B^{(\pm)} = \tfrac{1}{2}[\lambda_{11} - Z_{21}\lambda_{21} \pm Z_{12}(\lambda_{12} - Z_{21}\lambda_{22})],$$

the equations in Eq. (A1) can be transformed into the forms

$$A^{(+)}\eta + A^{(-)}\xi = 0, \quad (A4a)$$

$$B^{(+)}\eta + B^{(-)}\xi - \alpha a Q(\eta,\xi) = 0, \quad (A4b)$$

where the function $Q(\eta,\xi)$ is now given by

$$Q(\eta,\xi) = (2 - C)R_0\xi^2 + 4(x_0 - Z_{21}y_0 + 2\xi)R_0^2\xi^2 \equiv Q_0(\xi)\xi^2, \quad (A5)$$

$$R_0 = \frac{1}{2}\left[\frac{1}{x_0}\left(1 - \frac{A^{(-)}}{A^{(+)}}\right) + \frac{Z_{12}}{y_0}\left(1 + \frac{A^{(-)}}{A^{(+)}}\right)\right]. \quad (A6)$$

Thus with the new varaibles, $Q(\eta,\xi)$ becomes a function of ξ alone. The variable η may be easily eliminated from Eq. (A4b) since

$$\eta = -(A^{(-)}/A^{(+)})\xi. \quad (A7)$$

By substituting this into Eq. (A4b) and reorganizing the equation, we obtain

$$\xi[(A^{(+)}B^{(-)} - B^{(+)}A^{(-)})/A^{(+)} - \alpha a\xi Q_0(\xi)] = 0. \quad (A8)$$

This implies that either

$$\xi = 0 \quad (A9)$$

or

$$(A^{(+)}B^{(-)} - B^{(+)}A^{(-)})/A^{(+)} - \alpha a\xi Q_0(\xi) = 0. \quad (A10)$$

By substituting Eq. (A9) into Eq. (A7), we find the root

$$(\eta,\xi) = (0,0),$$

which means

$$(u_1,u_2) = (0,0)$$

for the steady state. This steady state is precisely the steady state (x_0,y_0). Equation (A10) is a quadratic equation since $Q_0(\xi)$ is linear with respect to ξ. Therefore, it is easy to obtain the roots of Eq. (A10) and ultimately the roots of Eqs. (A4a) and (A4b). They are as follows:

$$\eta^{(\pm)} = -(A^{(-)}/A^{(+)})\xi^{(\pm)}, \quad (A11a)$$

$$\xi^{(\pm)} = [q_0 \pm (q_0^2 + d_0)^{1/2}]/16R_0^2, \quad (A11b)$$

where

$$q_0 = (2 - C)R_0 + 4R_0^2(x_0 - Z_{21}y_0),$$

$$d_0 = 32R_0^2(A^{(+)}B^{(-)} - A^{(-)}B^{(+)})/A^{(+)}a\alpha.$$

The discriminant in Eq. (A11b) turns out to be negative for all values of $\alpha \geqslant 0$ for the parameter set chosen for the present work. Therefore, we conclude that there exists only one steady state for the present model of entropy production.

[1](a) B. C. Eu, J. Chem. Phys. **73**, 2958 (1980); (b) **74**, 6362 (1981); (c) **74**, 6376 (1981); (d) **80**, 2123 (1984); (e) Ann. Phys. (N.Y.) **140**, 341 (1982).

[2]N. Minorsky, *Nonlinear Oscillations* (Van Nostrand, Princeton, 1962).

[3]S. Glasstone, K. J. Laidler, and H. Eyring, *The Theory of Rate Processes* (McGraw–Hill, New York, 1941).

[4]B. C. Eu and A. S. Wagh, Phys. Rev. B **27**, 1037 (1983).

[5]B. C. Eu, Phys. Lett. A **96**, 29 (1983); J. Chem. Phys. **79**, 2315 (1983); Y. G. Ohr and B. C. Eu, Phys. Lett. A **101**, 338 (1984); B. C. Eu and Y. G. Ohr J. Chem. Phys. **81**, 2756 (1984).

[6]J. Ali and B. C. Eu, J. Chem. Phys. **80**, 2063 (1984).

[7]B. C. Eu, Phys. Lett. A **101**, 497 (1984).

[8]L. Onsager, Phys. Rev. **37**, 405 (1931); **38**, 2265 (1931).

[9]There are a number of observations and theoretical studies on current oscillation and fluctuation phenomena. For example, see I. L. Ivanov and S. W. Ryvkin, Sov. Phys. Tech. Phys. **3**, 722 (1958); R. D. Larrabee and M. C. Steele, J. Appl. Phys. **31**, 1519 (1960); M. Glicksman, Phys. Rev. **124**, 1655 (1961); C. E. Hurwitz and A. L. McWhorter, Phys. Rev. A **134**, 1033 (1964); J. B. Gunn, Solid State Commun. **1**, 188 (1963); S. Kabashima, H.

Yamazaki, and T. Kawakubo, J. Phys. Soc. Jpn. **40**, 921 (1976); M. Shaw, H. Grubin, and P. Solomon, *The Gunn–Hilsum Effect* (Academic, New York, 1979).

[10]P. H. Richter, P. Rehmus, and J. Ross, Prog. Theor. Phys. **66**, 385 (1981).

[11]Y. Termonia and J. Ross, Proc. Natl. Acad. Sci. U.S.A. **78**, 2952 (1981); **78**, 3563 (1981); **79**, 2878 (1982)..

[12]P. T. Landsberg, D. J. Robbins, and E. Schöll, Phys. Status Solidi A **50**, 423 (1978); **65**, 353 (1981).

[13]I. S. Gradshteyn and I. M. Ryzhik, *Tables of Integrals, Series, and Products* (Academic, New York, 1965).

[14]I. Prigogine, *Thermodynamics of Irreversible Processes* (Interscience, New York, 1967).

[15]P. Glansdorf and I. Prigogine, *Thermodynamic Theory of Structure, Stability, and Fluctuations* (Wiley, New York, 1971).

[16]R. Landauer observed in his analysis with circuits that the local equilibrium hypothesis for $d\mathcal{S}$ is admissible for systems in "the slowly modulated dissipative steady state" far from equilibrium; see R. Landauer, Phys. Rev. A **18**, 255 (1978). The words steady state and their implication must be stressed here as a limiter of his analysis. Note that Eq. (6.1) becomes the local equilibrium formula if the fluxes are steady in the frame moving with the fluid velocity, i.e., $d\hat{\Phi}_i^{(\alpha)}/dt = 0$.